Supporting Information "Direct near-field observation of surface plasmon polaritons on silver nanowires"

Matthias M. Wiecha[1], Shihab Al-Daffaie[2], Andrey Bogdanov[3], Mark D. Thomson[1], Oktay Yilmazoglu[2], Franko Küppers[4], Amin Soltani[1], Hartmut G. Roskos[1]*

[1]Physikalisches Institut, Goethe-Universität, D-60438 Frankfurt am Main, Max-von-Laue Str. 1, Germany

[2]Institut für Mikrowellentechnik und Photonik, TU Darmstadt, D-64283 Darmstadt, Merckstraße 25, Germany

[3]Department of Nanophotonics and Metamaterials, ITMO University, St. Petersburg 197101, Russia

[4]Skolkovo Institute of Science & Technology, Nobel st. 3, Skolkovo Innovation Centre, Moscow, 121205, Russia

1. Experimental setup. Our s-SNOM setup is a homebuilt AFM where the sample is scanned beneath the oscillating platinium coated tip (NanoWorld® ARROW^{TM} NCPt, resonance frequency ~ +-285 kHz; tapping amplitude set between 30-60 nm). The λ_0=853 nm near-IR laser (Toptica DL 100 DFB) is focused by an off-axis parabolic mirror (f=10 mm, N.A. ~ 0.2) onto the tip (~ 5.5 - 7.5 mW reaching the tip after the beam splitters; the higher values are for s-polarization measurements) and the scattered light is collected in backward direction via the parabolic mirror and guided to the detector. Using a Mach-Zehnder interferometer a pseudo-heterodyne detection scheme is implemented to suppress the background at the second and third harmonics of the cantilever oscillation Ω and to record both the electric field amplitude and phase (frequency pseudo-heterodyne mirror between 300-1000 Hz for different measurements). In our setup only two higher harmonics can be demodulated in parallel. Since the 3Ω data are already very noisy and we use the 2nd harmonic for quantitative analysis we omitted the 4th harmonic in the measurements. The NWs here are losing their s-SNOM response over a timescale of months; we assign this behavior to changes and chemical oxidation of the (unprotected) NW surface.

2. Simulation details. Dispersion curves and mode profiles in figure S7 were find numerically using COMSOL Multiphysics (Mode analysis module). The material parameters for the NW and substrate were taken from Refs. [1] and [2]. In this simulation we assume that the NW is infinitely long. This allows one separate the *y* variable (along the NW) and reduce the problem to 2D geometry. The diameter of the NW is assumed to equal to 200 nm. The electric field distribution in figure 2(c) were calculated using COMSOL Multiphysics (frequency domain module). Due the symmetry of the problem (in the case of s-polarized incident wave) we put perfect electric conducting plane perpendicular to the axis of the NW. The total length of the NW is assumed to equal to 4 μm.

3. Details on the fitting of the experimental data. Here, we present the models and equations used to fit the data for the p-polarization and the s-polarization measurement. Both polarizations are the sum (equations (S1) and (S2)) of two different modes. In (S1) a background field E_m is added (normal material s-SNOM signal of the NW). The s-polarization (S2) contains an arbitrary offset E_0. It is mathematical identical to E_m in (S1), but actually there should not be any material contrast for s-polarization. Nevertheless, this term includes the experimental imperfections e.g. the coupling between the different polarization, improper alignment of polarization/NW … All the surface waves are shaped with a Gaussian function (with radius $\sigma_{p(s)}$) since the excitation spot is fixed to the scanning tip. $y_{p1(s1)}$ is the fixed y-coordinate of the launching NW edge. The observable pattern in the p-polarization measurement is longer since the Gaussian shape is projected onto the NW axis (see also figure 2a and 2b or mathematical it is implemented within the cosθ factor in equation S3).

$$E_{total}^{p-pol}(y) = real(E_m + (mode_{p1} + mode_{p2}) * e^{-(\frac{y-y_{p1}}{\sigma_p})^2}) \quad \text{(S1)}$$

$$E_{total}^{s-pol}(y) = real(E_0 + (mode_{s1} + mode_{s2}) * e^{-(\frac{y-y_{s1}}{\sigma_s})^2}) \quad \text{(S2)}$$

All modes possess an own amplitude $E_{p1(p2,s1,s2)}$, k-vector $k_{1(2)}$, damping constant $\alpha_{1(2)}$ and phase offset $\phi_{p1(p2,s1,s2)}$ (S3) and (S4). The $cos\theta$ factor in (S3) actually represents an entire angle factor of $cos\theta sin\phi$ since the NW alignment by hand is not perfectly parallel to the incoming light, so this factor calculates the projection onto the wire.

$$mode_{p1(p2)} = E_{p1(p2)} * e^{-i(((k_{1(2)} - k_0 \cos\theta)(y-y_1)) + \phi_{p1(p2)})} * e^{-\alpha_{1(2)}(y-y_1)} \quad \text{(S3)}$$

$$mode_{s1(s2)} = E_{s1(s2)} * e^{-i(k_{1(2)}(y-y_1) + \phi_{s1(s2)})} * e^{-\alpha_{1(2)}(y-y_1)} \quad \text{(S4)}$$

The k-values from the COMSOL simulations are considered as constants whereas all other parameters are optimized as free parameters by the MATLAB fminsearch function or manually; the start parameters have to be chosen carefully to receive convincing results. The fitted α parameter are not very meaningful since the damping behavior is dominated by the Gaussian shape. Only data points within an interval from y_1 to y_2 are taken into account (equivalent to the NW geometry) and unphysical values are excluded (e.g. $\alpha_{1(2)}<0$). In the s-polarization measurement, the phase difference $|\phi_1 - \phi_2|$ between the two modes is close to π, i.e. the beating pattern starts close to the minimum of its envelope (therefore the signal is increasing from ~ 0 to 2 µm in e.g. Figure 1h). As mentioned before, we did not consider the reflection or SPP excitation from the opposite wire end. In the following, we show that excitation or reflection of the opposite end of the wire contradicts the experimental results.

For the p-polarization measurement, following equation (2) (with a plus sign) this would result in a Gaussian shaped short wavelength of ~450 nm on the opposite end. In the s-polarization case the measured wavelength would be identical to the SPP wavelength (since the electric field and not the intensity is mapped; only in the case of tip-emitted SPPs $\frac{\lambda}{2}$ is measured[3]). Both is not observed in the experiments shown in figure 1g and h. The minimum at ~7.5 µm in figure 1h is only an s-SNOM artifact (see as well figure 1f at the right end).

4. Supporting figures

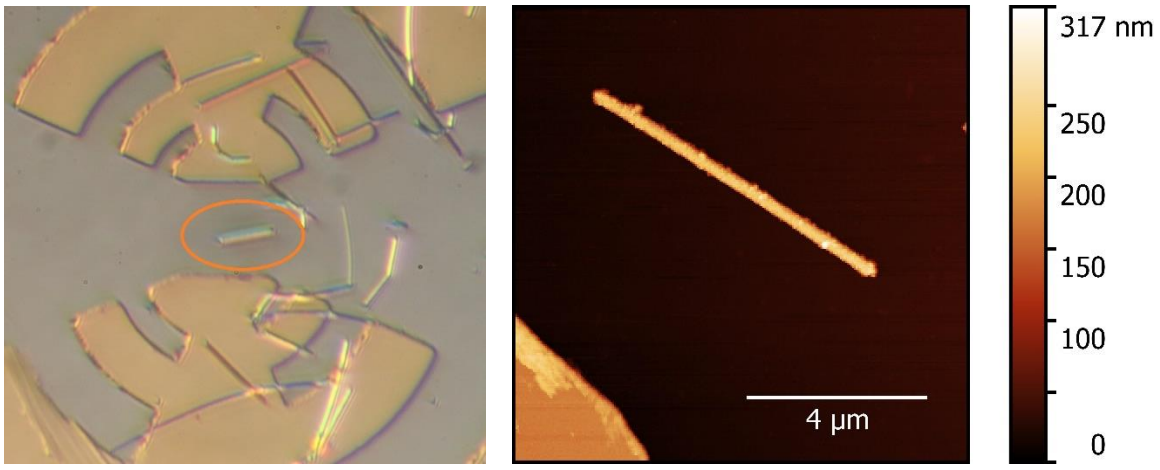

Figure S1. (left) Microscope image of arbitrarily distributed Ag-NWs on a LTG-GaAs substrate on which already a gold (Au) log-periodic antenna is fabricated to enable later the out-coupling of THz radiation during the THz generation. For this, the NW has to be re-positioned to touch an antenna arm. Due to their strong scattering, the NWs are even observable with a conventional light microscope. The orange marked Ag-NW is investigated in the paper since it has no (for s-SNOM measurements) disturbing connections to Au surfaces. (right) Entire AFM topography image of figure 1c (which is only a cutout) containing a part of the Au antenna that was used to align and confirm the s-SNOM signal. The dimension of this nanowire is ~211 nm * 7.5 µm (~diameter and length).

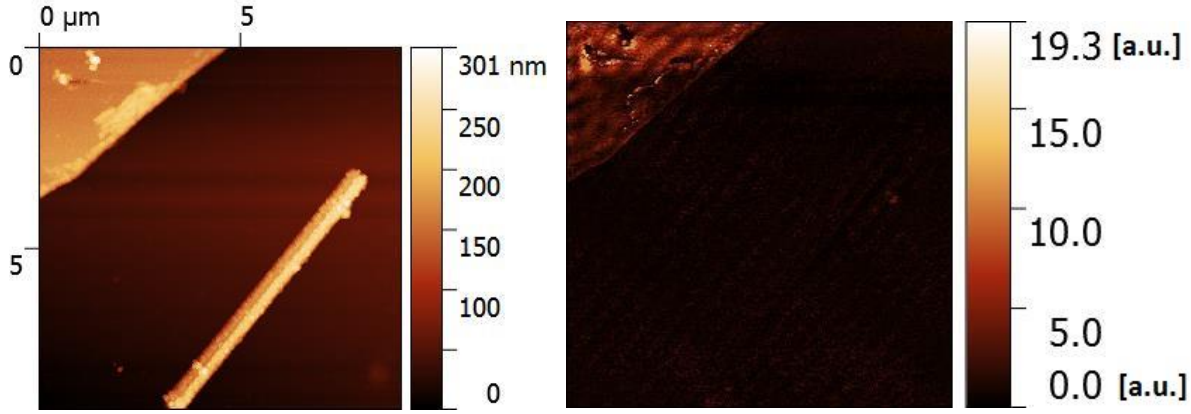

Figure S2. AFM topography (left) and 3Ω s-SNOM image (right) of an Ag NW with p-polarized light. The incident direction is from the upper left; therefore there is (almost) no field component parallel to the NW and no plasmons are excited on the NW. This measurement correspond to the p-polarization measurement in the main paper (figure 1 left column) with a ~90° rotated sample.

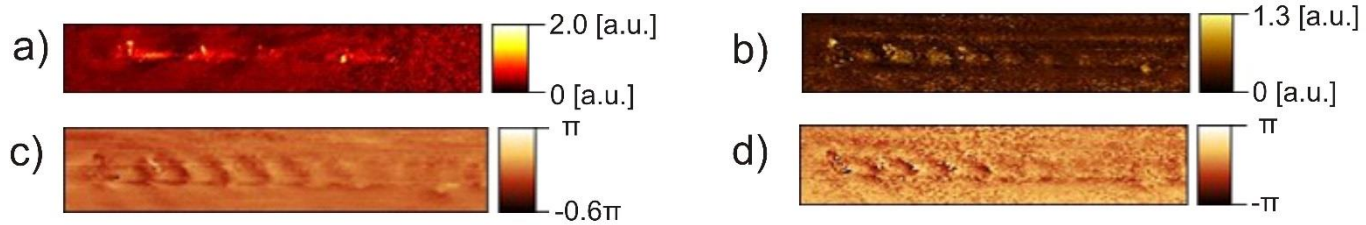

Figure S3. (a+b) The additional 3Ω s-SNOM measurements recorded in parallel to figure 1c+e and 1d+f, respectively show the same pattern as the 2Ω and confirm the results due to their increased background suppression. (c+d) The phase images of the s-polarization measurement figure 1f at (c) 2Ω and d) 3 Ω) confirms our interpretation.

Figure S4. Although the nanowire is symmetrical, due to the incident light the excitation at both ends differs resulting in a much stronger SPP excitation here at the left side. The E-field (oscillating in the yz-plane) can move electrons in both directions as it "sees" the entire front facet; on the right side it is "shadowed" by the nanowire itself.

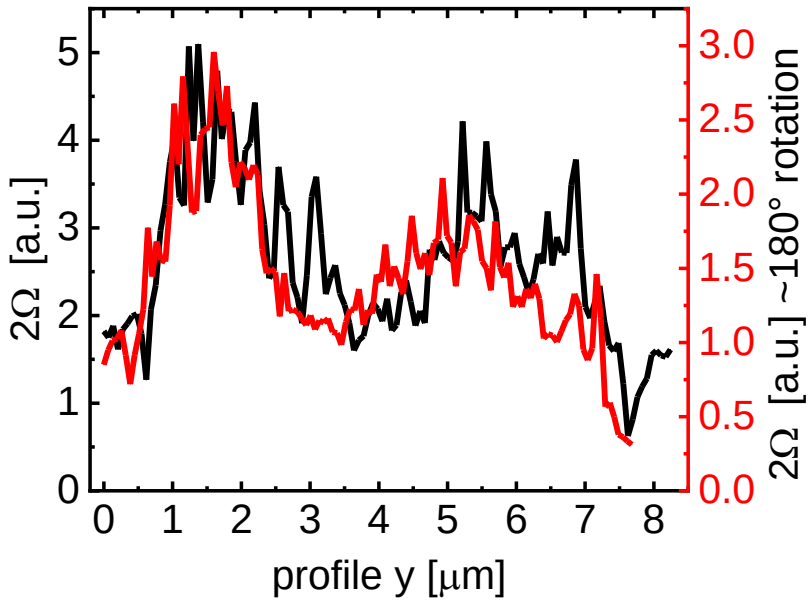

Figure S5. s-SNOM measurements on a (different) nanowire with p-polarization (geometry corresponding to figure 1a). The sample was rotated by ~180°, which results in a comparable pattern (excitation for both graphs from the left side). This confirms that not the structure of the two end facets is responsible for the different SPP launching, but rather the excitation geometry stated in figure S4 itself. The deviation in those two measurements is due to misalignment of the ~180° rotation by hand.

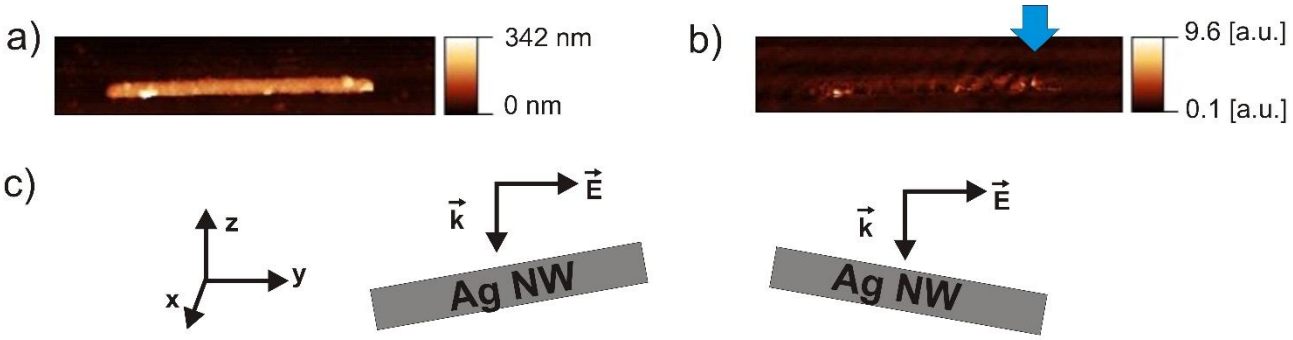

Figure S6 (a+b) Another s-polarization s-SNOM measurement (equivalent to figure 1 right column; (a) AFM topography (b) 2Ω pseudo-heterodyne s-SNOM) on another nanowire shows a tilted wave pattern as well. Since the signal is much weaker, it was not considered for quantitative analysis. Nonetheless, the orientation of the pattern is different and it is located at the opposite end of the wire (with respect to the incident light). This confirms the argument in the paper of non-symmetric excitation. (c) Depending on the exact orientation of the NW axis with respect to the incident light the asymmetry stated in S4 occurs again for s-polarization (E-vector parallel to y-axis; k-vector within xz-plane).

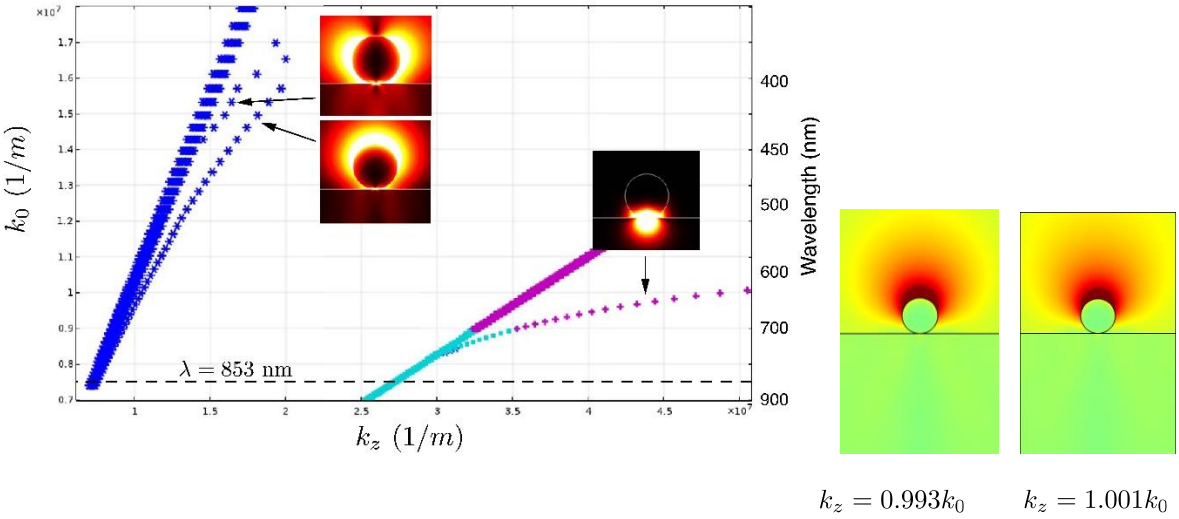

Figure S7. (left) Dispersion diagram of an Ag NW on a GaAs substrate. The data show two confined mode close to the light line in air and one mode close the light line in the substrate. Since the s-SNOM is probing the surface from above, we do not consider the latter one and are using the two modes from the left branch which are quite close to each other at 853 nm (852 nm and 859 nm, see the mode pictures to the right).

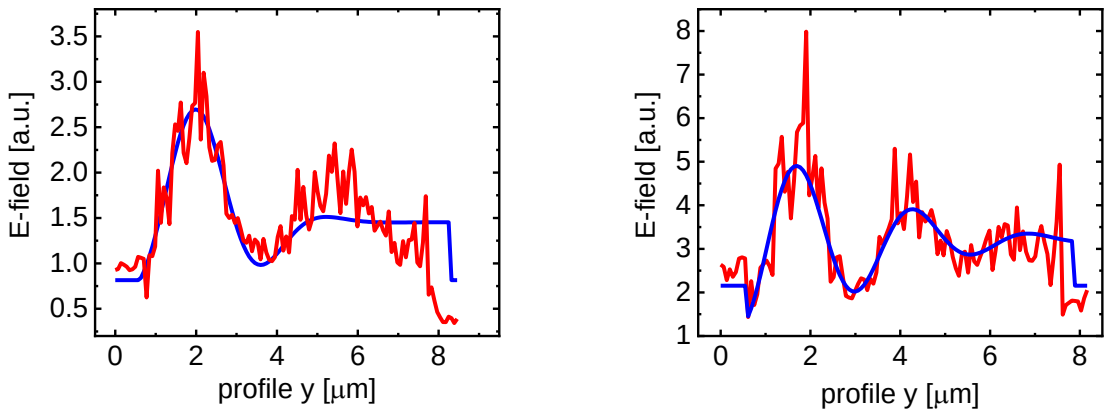

FIGURE S8. 2Ω s-SNOM linescan (red) and fitting (blue) of another nanowire with λ_0 = 853 nm (left) and λ_0 = 780 nm (right). The incident laser direction is again from the left side. For the shorter 780 nm, one can observe how the pattern is narrower and even a weak third bump is emerging. The quantitative results are not comparable with the main paper since another NW was used (different geometry, etc.). The lower available laser power and increased signal-to-noise ratio of the λ_0 = 780 nm device (Cheetah DFB-laser from Sacher laser) are not suitable for s-polarization measurements. Even for the λ_0 = 853 nm measurement the noise-level is higher than figure 1g+h since the sample is older.

References

(1) P.B. Johnson; R.W.Christy. PhysRevB.6.4370. *Phys. Rev. B* **1972**, *6* (12), 1–10. https://doi.org/10.1103/PhysRevB.6.4370.

(2) Adachi, S. Optical Dispersion Relations for GaP, GaAs, GaSb, InP, InAs, InSb, Al XGa1-XAs, and In1-XGaxAs YP1-Y. *J. Appl. Phys.* **1989**, *66* (12), 6030–6040. https://doi.org/10.1063/1.343580.

(3) Fei, Z.; Rodin, A. S.; Andreev, G. O.; Bao, W.; McLeod, A. S.; Wagner, M.; Zhang, L. M.; Zhao, Z.; Thiemens, M.; Dominguez, G.; et al. Gate-Tuning of Graphene Plasmons Revealed by Infrared Nano-Imaging. *Nature* **2012**, *487* (7405), 82–85. https://doi.org/10.1038/nature11253.